International Journal on Electrical Engineering and Informatics - Volume 17, Number 1, March 2025

Optimal sizing of Stand-Alone Photovoltaic system by minimizing the Loss of Power Supply Probability using Meerkat Optimization Algorithm

Mazwin Mazlan[1,2], Shahril Irwan Sulaiman[1*], Azralmukmin Azmi[2], Hedzlin Zainuddin[3] and Ismail Musirin[1]

[1]School of Electrical Engineering, College of Engineering, Universiti Teknologi MARA, 40450 Shah Alam, Selangor, Malaysia
[2]Faculty of Electrical Engineering Technology, Universiti Malaysia Perlis, 02600, Arau, Perlis, Malaysia
[3]Faculty of Applied Sciences, Universiti Teknologi MARA, 40450 Shah Alam, Selangor, Malaysia
*Corresponding author: shahril_irwan2004@yahoo.com

Abstract: The increasing demand for reliable and sustainable energy in off-grid areas has driven the need for efficient Stand-Alone Photovoltaic (SAPV) system designs. One of the key challenges in SAPV implementation is determining the optimal configuration of system components to ensure high reliability and cost-effectiveness. Conventional methods such as the Iterative-Based Sizing Algorithm (ISA) can achieve accurate sizing but are computationally intensive, especially when evaluating a large number of component combinations. This study proposes a Meerkat Optimization Algorithm-based Sizing Approach (MOA-SA) as an alternative method to improve sizing efficiency for SAPV systems. The objective is to minimize the Loss of Power Supply Probability (LPSP) while significantly reducing computation time. The methodology involves applying MOA-SA to two system configurations: one with a PV array, battery and hybrid inverter (System 1) and another with a PV array, battery, charge controller and solar inverter (System 2). The results showed that MOA-SA successfully achieved the optimal LPSP in all design cases with faster computation time and outperformed other sizing algorithms to meet load demand of a school in Pos Musoh, Perak, Malaysia.

Keywords: Meerkat Optimization Algorithm, Stand-Alone Photovoltaic, Loss of Power Supply Probability (LPSP)

1. Introduction

With the increased concern of the whole world for sustainable development and conservation of the environment, demands are arising for renewable energy applications. Therefore, solar power is an important factor for the shift towards cleaner energy. Stand-Alone Photovoltaic systems, dependent on solar energy, are a good option apart from conventional remote and off-grid areas. Ecologically, SAPV systems reduce the emission of greenhouse gases and help in conserving critical finite resources of fossil fuel. In their potential to produce clean energy, they meet Sustainable Development Goal 7: Affordable and Clean Energy-intended to ensure access to affordable, reliable, sustainable and modern energy for all. The optimization of efficiency and reliability in SAPV systems involves a proper balance between energy generation and storage to minimize power shortages. Therefore, the optimal sizing of the components of the system means ensuring the performance and sustainability of the system. [1], [2]. Empirical research has been conducted with the aim of devising a method for the optimal sizing of the photovoltaic system to balance energy production and consumption.

One of the most important definitions in this respect is that of Loss of Power Supply Probability, relating to the possibility of an SAPV system not being able to supply energy at any instant of time. The LPSP minimization is highly necessary for the purpose of continuity in energy availability, especially in those regions where solar irradiance is intermittent. LPSP minimization and hence the optimization of system component sizing, such as the photovoltaic panels, batteries, and inverters, has been performed in previous works using different optimization techniques including genetic algorithms, particle swarm optimization methods, and iterative procedures. In addition, the design, simulation, and optimization of SAPV

Received: January 7th, 2025. Accepted: March 29th, 2025
DOI: 10.15676/ijeei.2025.17.1.6

systems have also been widely carried out by software tools such as HOMER Pro, PVSyst, and MATLAB/Simulink [3], [4].

These studies demonstrate that effective sizing strategies, which account for local solar patterns and load variability, can significantly improve system performance and reliability [5]. In the context of SAPV systems, optimizing the size of individual components is vital to prevent over-sizing, which leads to increased costs, or under-sizing, which compromises reliability. The general problem throughout any sizing optimization involves the trade-off between energy storage and generation, with each component requiring size optimization to avoid inflating system costs while meeting energy supply needs. This perspective is supported by [6], [7]. The main challenge lies in designing a system that minimizes the Loss of Power Supply Probability (LPSP) while reducing the use of unnecessary components.

Recent research has focused on developing optimization algorithms and modeling approaches that account for factors like solar irradiance variability, load demand, and economic feasibility. Studies show that techniques such as the Honey Badger Algorithm (HBA), Particle Swarm Optimization (PSO), and others effectively determine optimal component sizes by evaluating cost, reliability, and storage requirements simultaneously[8]–[12].

In SAPV systems, choosing component of inverter is critical due to each option's distinct impact on system functionality, efficiency, and adaptability [13]. Hybrid inverters, equipped with integrated battery management, allow seamless transitions among solar power, stored battery energy, and grid electricity (if available), thereby enabling energy storage and enhancing self-sufficiency [14]. This flexibility makes hybrid inverters ideal for applications focused on energy independence and efficient power usage across varying times and conditions.

Traditional solar inverters, by contrast, are solely optimized for converting DC energy from solar panels to AC power, offering higher efficiency for direct energy conversion and suiting setups where battery storage is unnecessary [15]. They present a cost-effective solution for PV systems where simplicity, lower costs, and ease of integration are prioritized over scalability and storage options [16], [17]. The choice of inverter type depends on immediate energy needs, budget, adaptability, and system independence goals. This study examines optimization techniques for two SAPV configurations: System 1 includes PV panels, a battery, and a hybrid inverter, while System 2 consists of PV panels, a battery, a charge controller, and a solar inverter. Both configurations aim to meet energy demands with minimal the Loss of Power Supply Probability (LPSP).

2. Methodology

The sizing of SAPV systems involves selecting the appropriate type, capacity, and configuration of key components such as the PV array, battery, inverter, and charge controller that the load demand can be met. This research focuses on design and sizing SAPV system for a school in Pos Musoh, Perak, Malaysia located at approximately 4.26515°N, 101.40331°E. The school comprises various facilities, including six classrooms, five laboratories, a canteen, an administrative office, restrooms and a prayer room (surau). Table 1 illustrates the daily load profile of the school during school days and public holidays. Since the sizing is conducted to meet the load demand for one school, a PV-battery system is considered.

In this study, two system configurations were analyzed: System 1, comprising a PV array, battery, and hybrid inverter; and System 2, consisting of a PV array, battery, charge controller, and solar inverter. To evaluate the performance of each configuration, the LPSP was used as the primary reliability indicator. Firstly, the sizing of SAPV system was initiated with the formulation of Conventional Sizing Algorithm (CSA). CSA is capable of sizing system with only single set of system components. Later, an Iterative-Based Sizing Algorithm (ISA) was developed to enable the evaluation of multiple models for each system component, thereby facilitating a more flexible and realistic sizing process. This approach reflects common engineering practice, where various design alternatives are explored prior to selecting the optimal solution. In addition to supporting optimal component selection, the results produced by ISA are also utilized as a benchmark for evaluating the performance of the proposed Meerkat Optimization Algorithm-based sizing approach (MOA-SA).

Table 1. The estimated daily load profile

Usage		Appliances	Power per unit	Power factor	Total Number of units	Usage time (Monday - Thursday)	Energy (Monday - Thursday)	Usage time (Friday)	Energy (Friday)	Usage time (Weekend / School holidays)	Energy (Weekend / School holidays)
		240Vac, 50hz	W			h	VAh	h	VAh	h	VAh
(i) Classroom activity	Classrooms & Labs	Florescent lamps	32	1	48	2	3072.00	2	3072.00	0	0.00
		Ceiling Fan	72	0.92	14	3.5	3834.78	0.75	821.74	0	0.00
	Kitchen & canteen	Florescent lamps	32	1	8	3	768.00	3	768.00	0	0.00
		Wall Fan	59	0.98	9	2	1083.67	0.75	406.38	0	0.00
		Blander	350	0.8	1	0.5	218.75	0.5	218.75	0	0.00
	School office	Florescent lamps	32	1	17	2	1088.00	2	1088.00	0	0.00
		Ceiling Fan	72	0.92	9	4	2817.39	1.25	880.43	0	0.00
		Air conditioner	870	0.8	1	0.5	543.75	0	0.00	0	0.00
		TV	48	1	1	0.5	24.00	0	0.00	0	0.00
		Decoder NJOI	24	0.98	1	0.5	12.24	0	0.00	0	0.00
		CPU	280	0.95	2	2.75	1621.05	0.88	518.74	0	0.00
		Monitor	16	0.95	2	2.75	92.63	0.88	29.64	0	0.00
		Printer	10	0.9	2	1	22.22	0.5	11.11	0	0.00
		Mobile phone charger	15	0.9	5	1	83.33	0.4	33.33	0	0.00
		Microwave	800	0.8	1	0.5	500.00	0	0.00	0	0.00
		Kettle	2200	0.85	1	0.5	1294.12	0.5	1294.12	0	0.00
	Toilets	Florescent lamps	32	1	7	0.5	112.00	0.5	112.00	0	0.00
(ii) Surau activity (for community)	Subuh, Zohor, Asar, Magrib, Isya and quran recitation class	Horn speaker	50	0.95	2	0.167	87.89	0.167	87.89	0.167	87.89
		Amplifier	660	0.95	1	0.167	580.11	0.167	580.11	0.167	580.11
		Incandescent light bulb	20	1	10	3.167	633.40	3.167	633.40	3.167	633.40
		Wall Fan	59	0.98	6	4.33	1564.10	4.33	1564.10	4.33	1564.10
(iii) Others	Corridor lamps	Florescent lamps	32	1	22	12	8448.00	12	8448.00	12	8448.00
	Guardroom	Florescent lamps	32	1	1	12	384.00	12	384.00	12	384.00
		Wall Fan	59	0.98	1	12	722.45	12	722.45	12	722.45
		Mobile phone charger	15	0.9	1	2	33.33	2	33.33	2	33.33
Total							29641.23		21707.53		12453.28

A. Conventional-based sizing algorithm approach

The conventional sizing of SAPV system is conducted using a prescribed sizing procedure. In this study, CSA was developed in Matlab. The CSA initially requires the system designer to select a set of system components for System 1 and System 2 before trying to match the characteristics of the system components. After that, the expected performance indicator LPSP for SAPV system is computed. The technical sizing procedure for CSA primarily involves several steps in determining the system configuration that is expected to to meet the load demand. The sizing procedure is summarized as follows [11], [18]:

Step 1: Select and determine the sizing components for System 1 and System 2.
Step 2: Obtain the load profile of the site being used is shown in Table 1.
Step 3: Determine the total required load demand, E_{req_daily} in VAh by using,

$$E_{req\_daily} = \frac{E_{AC}}{\eta_{inv}} \tag{1}$$

where E_{AC} is total daily load demand in Vah and η_{inv} is the efficiency of the inverter.

Step 4: Determine the irradiation-to-load ratio, R_{IL} to find the worst month where H_{poa} is the average daily solar irradiation as shown in Table 2. The worst month is determined by selecting the month with the lowest R_{IL}.

$$R_{IL} = \frac{H_{poa}}{E_{req\_daily}} \tag{2}$$

Table 2. Average daily irradiation since January 1984 until December 2013 [19].

Month	Jan	Feb	Mac	April	May	June	July	August	Sept	Oct	Nov	Dec
Irradiation, G (kWh/m^2)	4.05	4.59	4.32	4.3	4.08	4.18	4.02	3.52	3.34	3.3	3.15	3.3

Step 5: Determine the System Voltage (SV) based on the system's daily energy requirement (E_{req_daily}). The appropriate SV is selected according to the values shown in Table 3.

Table 3. Criteria for selecting SV (S.Shaari et al.2014)

Condition	**Recommend SV, in V**
Condition 1: $E_{req\ daily} \leq 1k\ Wh$	12V
Condition 2: $1.001k\ Wh \leq E_{req\ daily} \leq 2k\ Wh$	24V
Condition 3: $2.001k\ Wh \leq E_{req\ daily} \leq 4k\ Wh$	48V
Condition 4: $4.001k\ Wh \leq E_{req\ daily} \leq 8k\ Wh$	96V

Step 6: Determine the required Ah demand of the battery bank, $C_{req\ batt}$ in Ah using,

$$C_{req\_batt} = \frac{E_{req\_daily}}{SV} \times \frac{T_{aun}}{DOD_{max}} \tag{3}$$

where T_{aun} is the required number of autonomy days of the battery bank and basically set between 5 and 10 days [21]. The DOD_{max} is the maximum allowable depth of discharge of the battery bank and it is set to 80%.

Step 7: Determine the required capacity of revised battery bank, $C_{rev\ batt\ req}$ in Ah using

$$C_{rev\_batt\_req} = \frac{C_{req\_batt}}{f_{temp\_batt}} \tag{4}$$

where $f_{temp\ batt}$ is the battery temperature correction factor and it is set to 0.98.

Step 8: Determine the total discharge current from the battery bank, $I_{bank\ disch}$ using

$$I_{bank\_disch} = \frac{1}{SV} \times \sum_{1}^{z} \frac{P_{AC}}{PF} \tag{5}$$

where z is the load number, P_{AC} is the power rating of particular load and PF is the power factor of the load. Addition, the discharge rate of the battery bank in hours is calculated using

$$T_{bank\_disch} = \frac{C_{rev\_batt\_req}}{I_{bank\ disch}} \tag{6}$$

Step 9: Determine the battery bank configuration. The number of batteries per string, $N_{series\ batt}$, and number of parallel strings of batteries, $N_{parallel\_batt}$ using

$$N_{series\_batt} = \frac{SV}{V_{nom\_battery}} \tag{7}$$

$$N_{parallel\_batt} = \frac{C_{rev\_batt\_req}}{C_{per\_batt}} \tag{8}$$

where $V_{nom\_battery}$ is the nominal battery voltage and C_{per_batt} is the Ah capacity of the battery at the discharge rate.

Step 10: The PV array configuration for MPPT charge controller:

i. The total number of PV modules, N_{total_PV} to meet the energy demand using

$$N_{total\_PV} = \left[\frac{E_{req\_daily} \times f_o}{P_{mp\_stc} \times PSH \times \eta_{PV\ ss}}\right] \tag{9}$$

where P_{mp_stc} in Wp represents the rated maximum power at Standard Test Conditions (STC), PSH denotes the peak sun hour, $\eta_{PV\ ss}$ is the sub-system efficiency from PV array to charge controller in decimals while f_o represents a growth factor for the load.

ii. The total number of PV array for each controller using MPPT charge controller, $N_{total\_PV\_per\_CC}$ using:

$$N_{total\_PV\_per\_CC} = \left[\frac{P_{nom} \times f_o}{P_{mp\_stc} \times sf1}\right] \tag{10}$$

where P_{nom} is the nominal power of charge controller in W and $sf1$ is safety factor and it is set to 1.2.

iii. The maximum series per charge controller.

$$N_{series\_max} = \left[\frac{V_{max\_cc} \times sf1}{V_{oc\_max}}\right] \tag{11}$$

$$V_{oc\_max} = V_{oc\_stc} \times \left(1 + \left[\frac{\beta_{voc}}{100} \times \left(T_{cell\_min} - 25^{\circ}\mathrm{C}\right)\right]\right) \tag{12}$$

where $V_{max\ \ cc}$ is maximum allowable input voltage to charge controller in V and $V_{oc\ max}$ is the maximum open circuit voltage of PV module in V and $V_{oc\ stc}$ is the open circuit voltage at STC. In this $T_{cell\ min}$ is the expected minimum operating cell temperature in ºC is set to be 20 ºC, β_{voc} is temperature coefficient for open circuit voltage in % per ºC and 25ºC is set for the cell temperature at standard test condition.

iv. Total number of charge controllers.

$$N_{total\_CC} = \left[\frac{N_{total\_PV}}{N_{Total\_PV\_per\_CC}}\right] \tag{13}$$

Step 11: Compute the required minimum power of inverter based on maximum power, $P_{max\ \ req\ inv}$ in VA using and required minimum power of inverter based on surge power, $P_{surge\ \_load}$ in VA using

$$P_{max\ \ req\ inv} = P_{max\ \ load} \times f_{ov} \tag{14}$$

$$P_{surge\_req\_inv} = P_{surge\ \_load} \times f_{ov} \tag{15}$$

where f_{ov} represent the oversized factor of inverter to consider load growth, $P_{max\ \ load}$ is the maximum AC load demand while $P_{surge\ \_load}$ is the surge demand of the load in VA.

To assess the performance of the system, the Loss of Power Supply Probability (LPSP) serves as a key reliability metric. LPSP quantifies the system's ability to meet load demand, representing the proportion of the total demand that cannot be satisfied by the power supply.

Step 12: Determine the energy output of the PV generator during an hour, $E_{PV}(n)$ in using;

$$E_{PV}(n) = P_{array\ stc} \times PSH(n) \times f_{temp}(n) \times f_{mm} \times f_{dirt} \times \eta_{cable} \times \eta_{inv} \times \eta_{cc} \times \eta_{batt} \tag{16}$$

where P_{array_stc} is the maximum power of the PV array at STC in W, $PSH(n)$ is the peak sun hour in hours, f_{mm} is the reduction factor due to mismatch of power on PV modules, f_{dirt} is the factor of dust and dirt accumulation on PV modules, η_{cable} is the efficiency of cabling set as 95%, η_{cc} is efficiency of charge controller, η_{batt} is the efficiency of battery and $f_{temp}(n)$ is the derating factor of power due operating temperature and can be calculated using;

$$f_{temp}(n) = 1 + \left[\beta_{Pmp} \times \left(T_{cell}(n) - T_{stc}\right)\right] \tag{17}$$

$$T_{cell}(n) = T_a(n) + \left(\frac{NOCT - 20}{800}\right) \tag{18}$$

where β_{Pmp} is temperature coefficient for maximum power in % per ºC, $T_{cell}(n)$ represents the PV panel temperature in °C, T_{stc} is the temperature at standard test conditions, set at 25°C, $T_a(n)$ is the ambient temperature on an hour in °C and $NOCT$ refers to the Nominal operating cell temperature set at 45°C. The constant value 20 is used to normalize the NOCT temperature to a baseline and 800 represents the reference solar irradiance in W/m^2.

Step 13: Determine the net energy content of the battery bank on an hour *n*, $E_{batt}(n)$. If $E_{PV}(n)$ is greater than the load demand of an hour *n*, $E_{load}(n)$, the battery bank will be charged to store the excess energy using

$$E_{batt\_charge}(n) = E_{batt}(n-1)(1-\sigma) + \left(E_{PV}(n) - \frac{E_{load}(n)}{\eta_{inv}}\right)\eta_{batt} \tag{19}$$

where $E_{batt}(n-1)$ is the previous amount of the battery capacity in kWh, σ is the battery self-discharge rate.

On the other hand, if $E_{load}(n)$ is greater than the load demand of an hour *n*, the battery bank will be discharging using

$$E_{batt\_discharge}(n) = E_{batt}(n-1)(1-\sigma) - \left(\frac{E_{load}(n)}{\eta_{inv}} - E_{PV}(n)\right)\eta_{batt} \tag{20}$$

$E_{batt}(n)$ is set to fulfill a constraint such that overcharging or undercharging of battery bank can be avoided. The constraint is

$$E_{batt\ min} \leq E_{batt}(n) \leq E_{batt\ max}$$

where $E_{batt\ min}$ is the minimum allowable energy level, preventing the battery bank from entering an over-discharged state. It is given by:

$$E_{batt\ min} = (1 - DOD_{max}) \times N_{parallel\ batt} \times C_{per\ batt} \times V_{nom\ battery} \tag{21}$$

$E_{batt\ max}$ is the maximum allowable energy content, representing the fully charged state of the battery bank:

$$E_{batt\ max} = N_{parallel\ batt} \times C_{per\ batt} \times V_{nom\ battery} \tag{22}$$

If the $E_{batt}(n)$ exceeds $E_{batt\ max}$, it is set to $E_{batt\ max}$, indicating a fully charged condition. Conversely, if $E_{batt}(n)$ falls below $E_{batt\ min}$, it is constrained to $E_{batt\ min}$, ensuring protection from excessive discharge and subsequent damage. This approach maintains the battery within optimal limits, enhancing longevity and operational efficiency.

Step 14: Calculate the LPSP using

$$LPS(n) = E_{load}(n) - (E_{PV}(n) + E_{batt}(n-1) - E_{batt\ min}) \times \eta_{inv}) \tag{23}$$

$$LPSP = \frac{\sum_{n}^{N} LPS(n)}{\sum_{n}^{N} E_{load}(n)} \tag{24}$$

B. Iterative-based sizing (ISA) approach

The CSA is limited to operating with a specific set of system components. When alternative component combinations are introduced into the design, the sizing process must be repeated. To address this limitation, [22] developed the Iterative-based Sizing Algorithm (ISA), which automates the selection process by optimizing the configuration of system components. ISA effectively reduces the need for repetitive manual resizing by streamlining the identification of optimal component sets. This approach aligns with current trends in renewable energy systems design, where automated optimization algorithms are essential for reducing complexity and improving overall efficiency [23]–[25].

In this study, individual component databases were created in Microsoft Excel for easy maintenance and integration with Matlab, covering PV modules, batteries, hybrid inverter, charge controllers and solar inverters. Each database contains ten models categorized by technical specifications. PV module parameters include maximum power at Standard Test Conditions (STC), *Pmp_stc*, in Wp; voltage and current at maximum power, *Vmp_stc* in V and *Imp_stc* in A; open circuit voltage *Voc_stc,* in V, the temperature coefficient for open circuit voltage of PV module, *βVoc*, in % per C, the temperature coefficient for maximum power of PV module, *βPmp*, in % per C, the temperature coefficient for short circuit current of PV module, β_{Isc}, in % per C and reduction factor due to mismatch of power, f_{mm} in decimal. The battery parameters include nominal voltage, V_{nom_batt} in V, capacity of battery at 120h discharge rate, C_{batt_120h} in Ah, capacity of battery at 100h discharge rate, C_{batt_100h} in Ah, capacity of battery at 72h discharge rate, C_{batt_72h} in Ah, capacity of battery at 48h discharge rate, C_{batt_48h} in Ah, capacity of battery at 24h discharge rate, C_{batt_24h} in Ah, capacity of battery at 10h discharge rate, C_{batt_10h} in Ah and efficiency of battery, η_{batt} in %. The database of charge controller required for optimal sizing process are nominal voltage of charge controller, V_{nom_cc} in V, maximum input voltage of charge controller, V_{max_cc} in V, minimum input voltage to the MPPT of charge controller, $V_{min\_window\_cc}$ in V, maximum input voltage to the MPPT of charge controller, $V_{max\_window\_cc}$ in V, nominal power of charge controller, P_{nom_cc} in W, nominal output current charge controller, I_{nom_cc} in A, and efficiency of charge controller, η_{cc} in %. On the other hand, there are two separate lists of database inverter which were arranged according their power rating for solar inverter and database hybrid inverter. The specifications of solar inverter used for the optimal sizing process are nominal input voltage of inverter, V_{nom_inv} in V, continuous power of inverter, $S_{continous\_inv}$ in VA, maximum power of inverter, $S_{maximum\_inv}$ in VA, surge power of inverter, S_{surge_inv} in VA, and efficiency of inverter, η_{inv} in %. The hybrid inverter database combines the specifications of both the solar inverter and the charge controller. For both systems, ten models were considered for each component and each model was an integer code. As a result, there were 1,000 possible component combinations for System 1 and 10,000 combinations for System 2 of system components that need to be evaluated in a particular sizing process. ISA based on System 1 and System 2 was developed to determine the optimal set of system components which produces the lowest LPSP. It implemented using the following steps:

Step 1: Load all the MS Excel databases include databases of components, load profile and solar irradiation into Matlab.
Step 2: Execute step 1 until step 4 in Section 2.1.
Step 3: Reconstruct each component database such that the selected SV is satisfied.
Step 4: Derive all possible combinations of system components from the databases.
Step 5: For each set of system components, execute step 5 until step 14 in Section 2.1 to determine LPSP.
Step 6: Identify the set of system components which produces the lowest LPSP. The optimal results for System 1 and System 2 have been benchmarks for MOA-based sizing algorithm.

C. Meerkat Optimization Algorithm (MOA)

The meerkat is a small, diurnal mammal with a brown-striped coat, commonly found in desert environments. It has a long tail used for balance when standing upright and distinctive black spots around its eyes that act like sunglasses, allowing it to see clearly in bright sunlight. Meerkats exhibit several unique behaviours. They use their sharp sense of smell to hunt small prey and communicate by purring. While some forage, others act as sentinels, scanning for predators and alerting the group with a warning cry if danger is detected. When threatened, meerkats may try to appear fierce by exposing their teeth and claws or standing together to mimic a larger animal. These behavioural patterns inspire the Meerkat Optimization Algorithm (MOA). The algorithm was formulated based on five idealized behavioural rules (Xian et al. 2023).

C.1. Establishment of initial populations

The initial population, X of MOA was first established using eq. (25), where represents the jth component of the ith prospect solution, i={1,2,…N} and j={1,2…,D}., represents the total number of individuals, and is the problem's dimension size.

$$X = \begin{bmatrix} X_{1,1} & X_{1,2} & \dots & X_{1,j} & \dots & X_{1,D} \\ X_{2,1} & X_{2,2} & \dots & X_{2,j} & \dots & X_{2,D} \\ \vdots & \vdots & \ddots & \vdots & \ddots & \vdots \\ X_{i,1} & X_{i,2} & \dots & X_{i,j} & \dots & X_{i,D} \\ \vdots & \vdots & \ddots & \vdots & \ddots & \vdots \\ X_{N,1} & X_{N,2} & \dots & X_{N,j} & \dots & X_{N,D} \end{bmatrix} \tag{25}$$

$$X_i^t = random_{normal}(loc = 0.5, sclae = 0.3) * (ub - lb) + lb \tag{26}$$

where $random_{normal}$ is distributed random number with standard deviation of 0.3 [26].

C.2. Hunting activities and vigilance

Meerkats adjust their behaviour based on the presence of predators and sentry warnings. In safe situations, when $rand < sentry$ threshold (default 0.3), they follow one of two strategies with equal probability: (i) searching for prey while staying alert by spreading out from their starting location, or (ii) approaching other meerkats for group hunting. These strategies depend on a probability, P (default 0.5), compared to a random value uniformly distributed. The strategies are mathematically formulated as follows:

$$X_i^{t+1} = \begin{Bmatrix} X_i^t + step * direct, & if\ P < rand, \\ X_i^t + step * \left(X_j^t - (rand + 0.5) * X_i^t\right), & otherwise, \end{Bmatrix} \tag{27}$$

$$\text{if}\ rand < sentry, \tag{28}$$

$$direct = X_i^0$$

$$step = \left(1 - {}^{t}/_{T}\right) * r \tag{29}$$

where X_i^{t+1} is the next position of the meerkat $(t + 1)$th iteration, and the current position at tth iteration is represented by X_i^t. When $P < rand$, meerkats expand their search outward from their initial position, *direct* looking for food and watching for predators. P is set to 0.5 by default to balance the two behaviour modes. The step size ($step$) decreases as the number of iterations increases, aiding in both global search and convergence.

In the other scenario, meerkats may randomly encounter other members of their group and join them for coordinated hunting, with Xj representing a randomly selected companion. The *rand* is a random number, t indicates the iteration's number, T denotes the maximum number of iterations, and r is a scaling factor.

C.3. Flee or fight against the enemy

In this strategy, the emergency is considered when $rand > sentry$. Meerkats are led to conduct reconnaissance for predators or natural calamities, and alerts are sent for others to either escape or defend themselves. Two scenarios are involved in this strategy: first, meerkats are gathered in the leader's direction, also known as the historical optimal global position, and positions are upgraded accordingly to give attackers the impression of a larger animal. In the second scenario, when the enemy is too powerful or escape routes are blocked, meerkats with poor fitness to the leader seek shelter in the opposite direction. The first scenario is represented mathematically when $f\left(X_{emergency}^t\right) < f(X_i^t)$, indicating better fitness value, while in the second scenario, the positions are upgraded or adjusted otherwise. Random bias (*div*) is employed to expand the population search, while leader direction is updated for quicker convergence.

$$X_i^{t+1} = \begin{cases} X_{emergency}^t & if\ f(X_{emergency}^t) < f(X_i^t), \\ div * X_i^t + (2 * rand * X_{gb}^t - X_i^t) & otherwise \end{cases} \quad (30)$$
$$if\ rand > sentry,$$

where,

$$X_{emergency}^t = X_i^t + (2 * rand * X_{gb}^t - X_i^t) \quad (31)$$
$$div = rand + 0.1 \quad (32)$$

C.4. Random direction exploration

At each iteration, the meerkats can explore random paths with the goal of finding paths which maximize food intake. These strategies help them never get stuck in local optima and let them find the very best food supplies. This process can be represented using mathematically as follows:

$$X_i^{t+1} = X_i^t + (2 * rand - 1) * (X_i^t * s) * step \quad (33)$$

where,

$$s = Levy\ flight\ step \quad (34)$$

C.5. Death and rebirth

When meerkats exceed the permitted boundaries, they are removed from the group. In such cases, it is necessary to regenerate new meerkats to preserve the population size, using the following equation:

$$X_i^{relocate} = random_{normal}(loc = 0.5, scale = 0.3) * (ub - lb) + lb \quad (35)$$

D. Meerkat Optimizer-based Sizing Algorithm (MOA-SA)

Figure 1 illustrates the operational flow of the Meerkat Optimization Algorithm (MOA) applied to the optimal sizing of SAPV system. The detailed development of MOA-SA for System 1 and System 2 are described as follows:

Step 1: Load all the MS Excel databases include databases of components, load profile and solar irradiation into Matlab.
Step 2: For each candidate solution, the fitness function is evaluated based on minimize LPSP.
Step 3: The MOA is executed. It simulates the behavioral traits of meerkats as described in Section 2.4.
Step 4. The population is updated iteratively over multiple generations. During each iteration, agents adapt their configurations based on the rules in Step 4 to improve LPSP outcomes.
Step 5: After each iteration, the algorithm checks if all candidate solution has converged or if the maximum number of iterations has been reached.
Step 6: Once convergence is achieved or the iteration limit is reached, the best performing solution is recorded as the optimal system configuration with minimize LPSP.

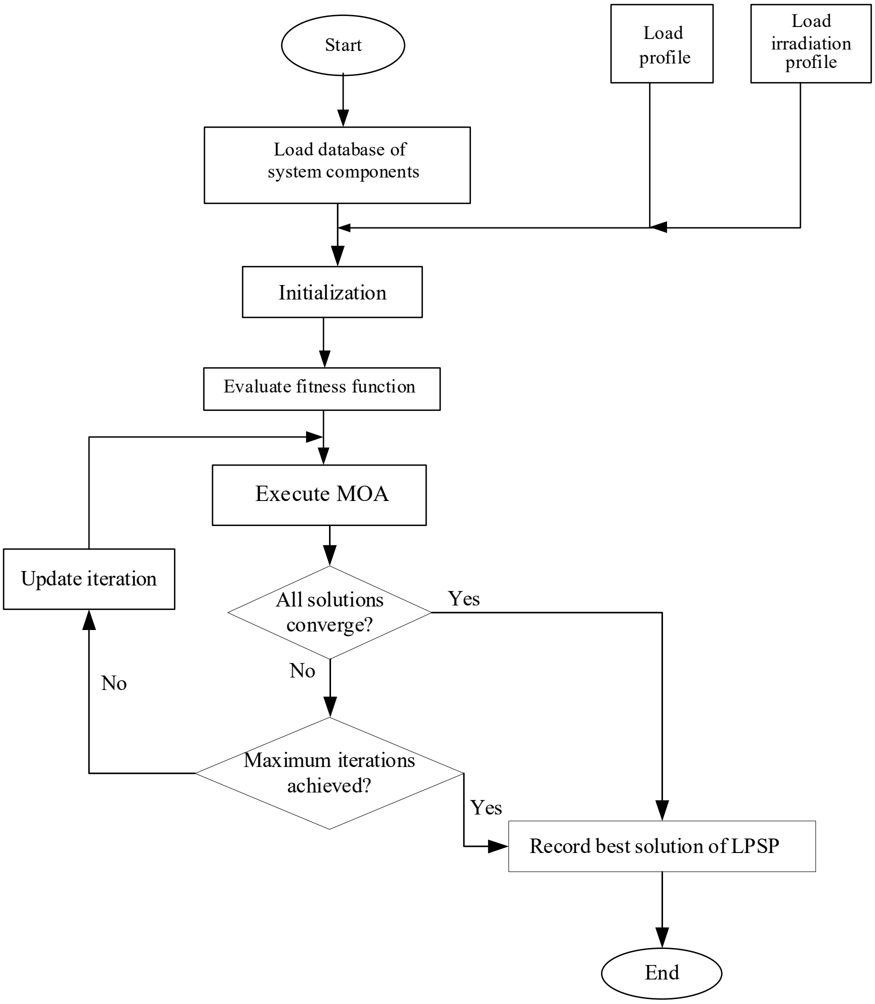

Figure 1. Flow chart of Meerkat Optimizer-based Sizing Algorithm (MOA-SA)

3. Result and discussion

The sizing results for ISA based on System 1 and System 2 are presented in Table 4. In System 1, the total computation time was found to be 466.23 seconds with 1000 sets of PV module, battery, and hybrid inverter being identified as valid solutions. A minimum LPSP of 0.045422 was achieved using code 4, code 4 and code 3 for PV module, battery and hybrid inverter respectively. Conversely, System 2 required 685.75 seconds of computation time, resulting in 10,000 sets of valid solutions. The minimum LPSP of 0.08329 in System 2 was obtained using code 4, code 10, code 1 and code 4 for PV module, battery, inverter and charge controller respectively. These LPSP values for both systems fall within the acceptable range for SAPV system in rural electrification applications in Malaysia as supported by related studies [8], [11]. Although the optimal PV module suggested is the same in both cases, the battery configuration differs significantly, with System 2 required a higher battery capacity to meet its energy needs. Consequently, distinct sets of sizing configurations and LPSP values are obtained, underscoring the necessity of investigating the sizing process using both systems. Next, several computational intelligence (CI) algorithms; MOA-SA, Particle Swarm Optimization (PSO), Firefly Algorithm (FA), and Slime Mould Algorithm (SMA) were applied to System 1 and System 2, with their parameter settings detailed in Table 5. For a realistic and reasonable comparison study, the number of populations and the maximum number of iterations were set for each technique is 20 and 30 respectively. The results from these intelligent optimization models are compared and benchmarked against ISA based on computation time and accuracy of the optimization.

Table 4. ISA sizing result of SAPV system for System 1 and System 2

Sizing results	System 1	System 2
Optimal PV module code	4	4
Optimal battery code	4	10
Optimal hybrid inverter code	3	-
Optimal inverter code	-	1
Optimal charge controller code	-	4
N_{series_PV} in integer	2	2
N_{total_PV} in integer	24	24
$N_{total\_PV\_per\_CC}$	10	10
N_{series_batt} in integer	4	4
$N_{parallel\_batt}$ in integer	19	81
N_{total_batt} in integer	76	324
$N_{total\_hybrid\_inv}$ in integer	5	-
$N_{total\_charge\_controller}$ in integer	-	3
N_{total_inv} in integer	-	2
Optimal Loss of Power Supply Probability (LPSP), dimensionless	0.045422	0.08329
Overall computation time, in seconds	466.23	539.65

Table 5. The parameter set of algorithms.

Algorithms	Parameters
MOA-SA	P = 0.1, sentry = 0.5, scale = 0.3
PSO	C1 = 0, C2 = 2[26]
SMA	Z = 0.03 [27]
FA	α = 0.5, β = 1, γ = 1 [27]

A. System 1 Analysis

Table 6 presents the numerical results of LPSP for System 1 across four optimization algorithms. The results for each algorithm include the best, mean, worst, and standard deviation (SD) values for LPSP across 20 runs. Importantly, MOA-SA displays the lowest standard deviation (0.00041), indicating minimal variability in its LPSP outcomes across runs. This stability is crucial for applications requiring reliable performance, as it demonstrates that MOA-SA consistently achieves near-optimal results. PSO, while attaining the same best LPSP value as MOA-SA, has a higher SD, suggesting more variation in its performance. In contrast, FA and SMA yield slightly higher LPSP values and greater SDs, indicating less reliable performance compared to MOA-SA and PSO.

Table 6. The numerical result of System 1 (LPSP)

Algorithm	Best	Mean	Worst	SD
MOA-SA	0.04542	0.04570	0.04690	0.00041
PSO	0.04542	0.05935	0.11063	0.02466
SMA	0.04563	0.05035	0.06161	0.00518
FA	0.04547	0.05276	0.10113	0.01399

Table 7 directly compares the best LPSP and computation time obtained by each algorithm on System 1 in minimization of LPSP. Here, MOA has resulted in the exact same optimal LPSP as that obtained with ISA in a much lower computation time of 1.1063 seconds and, hence is more than 420 times faster than ISA. PSO also performs impressively but takes a little more time, while FA and SMA result in higher LPSP values of 0.04573 and 0.04563, respectively, at higher computation cost. The low computation times of MOA-SA and PSO demonstrate the possibility of their usage in real-time applications, since they achieve optimal performance in terms of LPSP at reduced processing times. Figure 2 shows the convergence performance for each algorithm with the best fitness (LPSP) resulting over 30 iterations. The MOA-SA converges with much rapidity, finding the optimality of the LPSP in its five iterations as 0.04542 and explaining its efficiency by finding the optimal solution with rapid convergence.

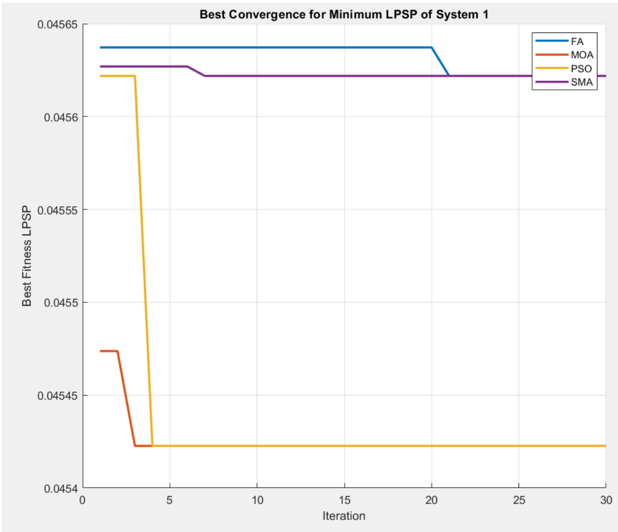

Figure 2. Performance of different algorithms for System 1

Table 7. Sizing performance of ISA, MOA-SA, PSO, SMA and FA in minimizing LPSP for System 1.

Sizing results	ISA	Optimization Techniques			
		MOA-SA	PSO	SMA	FA
Optimal Loss of Power Supply Probability (LPSP), dimensionless	0.04542	0.04542	0.04542	0.04563	0.04573
Overall computation time, in seconds	466.23	1.1063	1.8617	2.414	2.0216

B. System 2 Analysis

The numerical result for each algorithm applied to System 2, detailed in Table 8, include the best, mean, worst and standard deviation of LPSP. Consistent with System 1, MOA-SA demonstrates the lowest standard deviation (0.00013), underscoring its reliability and stability. This result is critical for applications needing consistent power reliability, as it suggests that MOA-SA can consistently achieve optimal outcomes with minimal variability. PSO, SMA, and FA show slightly higher variability, with greater standard deviations of 0.00145, 0.00133, and 0.00189, respectively, which indicates a broader range of LPSP results across runs.

Table 8. The numerical result of system 2 (LPSP)

Algorithm	Best	Mean	Worst	SD
MOA-SA	0.08329	0.08343	0.08374	0.00013
PSO	0.08329	0.08371	0.09121	0.00145
SMA	0.08329	0.08416	0.09010	0.00133
FA	0.08329	0.08420	0.09134	0.00189

Table 9 presents the computation times consumed by each algorithm to compute their optimal LPSP values in System 2. MOA-SA remains the fastest, with a computation time of only 4.776 seconds, compared to the 539.65 seconds of ISA. This significant cut in computation time proves the efficiency of MOA-SA and makes it one of the perfect choices when optimization needs to be done in the shortest time possible. PSO, SMA, and FA show moderate computation times, which can be considered feasible when the availability of computation resources or time is more flexible. Figure 3 presents a convergence behavior for each algorithm about System 2. It plots the best fitness obtained by each algorithm, LPSP in this case, over 30 iterations to demonstrate how each algorithm performs in convergence speed and the best solution quality it reaches. Due to the robustness of the optimization techniques employed, all the algorithms are able to reach the minimum of the LPSP. The speed of convergence may be explained by the nature of each algorithm. For example, MOA-SA and PSO are designed in such a way that they can explore and exploit the space with much better efficiency, and hence they converge comparatively faster towards the optimal solution. Contrarily, SMA and FA may focus more on the exploration of the solution space, despite the fact that convergence will be slower but does not readily fall into local optima.

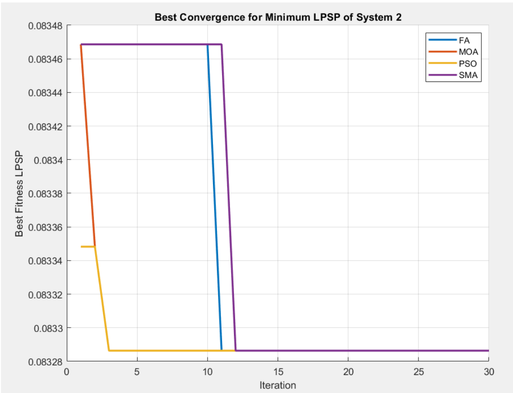

Figure 3. Performance of different algorithms for System 2

Table 9. Sizing performance of ISA, MOA-SA, PSO, SMA and FA in minimizing LPSP for System 2.

Sizing results	ISA	Optimization Techniques			
		MOA-SA	**PSO**	**SMA**	**FA**
Optimal Loss of Power Supply Probability (LPSP), dimensionless	0.08329	0.08329	0.08526	0.08547	0.08335
Overall computation time, in seconds	539.65	2.776	6.511	6.436	6.330

The template is used to format your paper and style the text. All margins, column widths, line spaces, and text fonts are prescribed; please do not alter them. You may note peculiarities. For example, the head margin in this template measures proportionately more than is customary. This measurement and others are deliberate, using specifications that anticipate your paper as one part of the entire proceedings, and not as an independent document. Please do not revise any of the current designations.

4. Conclusion

This paper introduces a new sizing algorithm using Computational Intelligence (CI) techniques for SAPV systems. Although the Iterative-Based Sizing Algorithm (ISA) is capable of finding the optimal design solution, it requires significant time to determine the combination of components during the optimization process. To address this issue, the MOA-SA was developed to accelerate the optimization process for SAPV systems. Studies have shown that both configurations in the SAPV system achieve significantly faster computation times compared to ISA. A comparison of CI techniques also demonstrates that MOA-SA achieves shorter computation times than PSO, FA, and SMA. In summary, MOA-SA is a practical sizing algorithm because it offers a more accurate and faster approach than existing optimization techniques for sizing SAPV systems.

5. Acknowledgement

The usage of facilities and financial assistance were greatly appreciated by the authors by the Universiti Teknologi MARA (UiTM), Universiti Malaysia Perlis (UniMAP) and Malaysia Ministry of Higher Education (MOHE).

6. References

[1] A. F. Ramos, I. Ahmad, D. Habibi, and T. S. Mahmoud, "Placement and sizing of utility-size battery energy storage systems to improve the stability of weak grids," *Int. J. Electr. Power Energy Syst.*, vol. 144, p. 108427, 2023.

[2] H. M. Ridha, C. Gomes, H. Hazim, and M. Ahmadipour, "Sizing and implementing off-grid stand-alone photovoltaic/battery systems based on multi-objective optimization and techno-economic (MADE) analysis," *Energy*, vol. 207, p. 118163, 2020.

[3] J. Lian, Y. Zhang, C. Ma, Y. Yang, and E. Chaima, "A review on recent sizing methodologies of hybrid renewable energy systems," *Energy Convers. Manag.*, vol. 199, no. April, p. 112027, 2019.

[4] S. Sinha and S. S. Chandel, "Review of software tools for hybrid renewable energy systems," *Renew. Sustain. Energy Rev.*, vol. 32, pp. 192–205, 2014.

[5] A. Khan *et al.*, "Enhanced Evolutionary Sizing Algorithms for Optimal Sizing of a Stand-Alone PV-WT-Battery Hybrid System," *Applied Sciences*, vol. 9, no. 23. 2019.

[6] T. M. Tawfik, M. A. Badr, O. E. Abdellatif, H. M. Zakaria, and M. EL-Bayoumi, "The Environmental and Economic Benefits of a Hybrid Renewable Energy System Considering Demand Side Management," *Int. J. Renew. Energy Res.*, vol. 12, no. 2, pp. 1063–1075, 2022.

[7] M. A. M. Khan, S. Rehman, and F. A. Al-Sulaiman, "A hybrid renewable energy system as a potential energy source for water desalination using reverse osmosis: A review," *Renew. Sustain. Energy Rev.*, vol. 97, pp. 456–477, 2018.

[8] N. A. Kamarzaman, S. I. Sulaiman, A. I. M. Yassin, I. R. Ibrahim, and H. Zainuddin, "A honey badger algorithm for optimal sizing of an AC coupled hybrid stand-alone photovoltaic system," *Energy Reports*, vol. 8, pp. 511–520, 2022.

[9] W. Nemouchi, Y. Amrane, and H. Nemouchi, *Optimal Sizing Design of stand- Alone Hybrid System Using a Fuzzy PSO*, vol. 361 LNNS. 2022.

[10] M. Usman, M. Tauseef, A. Singh, and S. Ali, "Techno-economic analysis of hybrid solar-diesel-grid connected power generation system," *J. Electr. Syst. Inf. Technol.*, vol. 5, no. 3, pp. 653–662, 2018.

[11] N. Izzati, A. Aziz, S. Irwan, S. Shaari, I. Musirin, and K. Sopian, "Optimal sizing of stand-alone photovoltaic system by minimizing the loss of power supply probability," *Sol. Energy*, vol. 150, pp. 220–228, 2017.

[12] O. Capraz, A. Gungor, O. Mutlu, and A. Sagbas, "Optimal sizing of grid-connected hybrid renewable energy systems without storage: a generalized optimization model," *Energy Sources, Part A Recover. Util. Environ. Eff.*, 2020.
[13] A. A. Salem, M. M. Ismail, H. A. Zedan, and B. E. Elnaghi, "Design of a perturb and observe and neural network algorithms-based maximum power point tracking for a grid-connected photovoltaic system," vol. 14, no. 4, pp. 3674–3687, 2024.
[14] A. A. Awad and M. Y. Suliman, "Energy management in stand-alone system based on solar/wind/batteries with an emergency diesel source," *AIP Conf. Proc.*, vol. 3232, no. 1, p. 50015, Oct. 2024.
[15] H. S. Kavitha, S. Mallikarjunaswamy, and N. Sharmila, "An Optimized Power Management System for Solar and Wind Energy Using Hybrid Inverters and Machine Learning," in *2024 Second International Conference on Networks, Multimedia and Information Technology (NMITCON)*, 2024, pp. 1–6.
[16] F. A. Khan, N. Pal, and S. H. Saeed, "Review of solar photovoltaic and wind hybrid energy systems for sizing strategies optimization techniques and cost analysis methodologies," *Renew. Sustain. Energy Rev.*, vol. 92, no. April, pp. 937–947, 2018.
[17] W. López-Castrillón, H. H. Sepúlveda, and C. Mattar, "Too many solar panels? Oversizing or undersizing of hybrid renewable energy systems based on different sources of information," *Sustain. Energy Technol. Assessments*, vol. 52, 2022.
[18] Z. Othman, S. I. Sulaiman, I. Musirin, A. M. Omar, and S. Shaari, "Hybrid Stand-alone Photovoltaic Systems Sizing Optimization Based on Load Profile," vol. 7, no. 2, 2018.
[19] "NASA Prediction Of Worldwide Energy Resources," 2022. [Online]. Available: https://power.larc.nasa.gov.
[20] N. Z. I. Z. Sulaiman Shaari, Maliki bin Omar, Shahril Irwan Sulaiman, *SEDA Malaysia Off-Grid Photovoltaic Systems Design Course*. SEDA Malaysia, 2014.
[21] N. I. Abdul Aziz, S. I. Sulaiman, S. Shaari, I. Musirin, and K. Sopian, "Optimal sizing of stand-alone photovoltaic system by minimizing the loss of power supply probability," *Sol. Energy*, vol. 150, pp. 220–228, 2017.
[22] N. Izzati, A. Aziz, S. I. Sulaiman, S. Shaari, and I. Musirin, "An Iterative Algorithm for Sizing Stand-Alone Photovoltaic System," vol. 785, pp. 601–605, 2015.
[23] Y. He, S. Guo, P. Dong, Y. Zhang, J. Huang, and J. Zhou, "A state-of-the-art review and bibliometric analysis on the sizing optimization of off-grid hybrid renewable energy systems," *Renew. Sustain. Energy Rev.*, vol. 183, 2023.
[24] S. Leva and E. Ogliari, "Computational Intelligence in Photovoltaic Systems," no. Lm, 2019.
[25] H. Rezk, M. Ali, and C. Ghenai, "Performance evaluation and optimal design of stand-alone solar PV-battery system for irrigation in isolated regions : A case study in Al Minya (Egypt)," *Sustain. Energy Technol. Assessments*, vol. 36, no. May, p. 100556, 2019.
[26] S. Xian and X. Feng, "Meerkat optimization algorithm: A new meta-heuristic optimization algorithm for solving constrained engineering problems," *Expert Syst. Appl.*, vol. 231, no. May, p. 120482, 2023.
[27] N. S. S. Mohamed, S. I. Sulaiman, S. R. Abdul Rahim, and A. Azmi, "Optimal sizing of a fixed-tilt ground-mounted grid-connected photovoltaic system with bifacial modules using Harris Hawks Optimization," *Energy Convers. Manag.*, vol. 314, no. June, p. 118738, 2024.

Mazwin Mazlan is currently a PhD student in Faculty of Electrical Engineering, Universiti Teknologi MARA, Malaysia. She received the B.Eng. degree in Industrial Electronic engineering from the Universiti Malaysia Perlis, Perlis, Malaysia, in 2010 and Master Engineering in Industrial Electronic and Control from Universiti Malaya in 2012. She is currently a Lecturer with the Faculty of Electrical Engineering Technology, Universiti Malaysia Perlis, Malaysia.

Shahril Irwan Sulaiman holds a PhD in Electrical Engineering from Universiti Teknologi MARA, Malaysia. He obtained his M.EngSc in Photovoltaic Engineering from University of New South Wales, Australia, and B.Eng in Electrical & Electronics from Universiti Tenaga Nasional, Malaysia. He is currently a senior lecturer in Faculty of Electrical Engineering, Universiti Teknologi MARA, Malaysia. His active contributions have been recognized when he is appointed as one of the Master Trainers by Sustainable Energy Development Authority (SEDA) Malaysia to conduct competency-based trainings related to design, installation, testing & commissioning, operation and maintenance of both gridconnected photovoltaic systems and stand-alone photovoltaic systems.

Azralmukmin Azmi (Member, IEEE) received the B.Eng. degree (Hons.) in electrical system engineering from the University Malaysia Perlis (UniMAP), in 2007, M.Eng. degree in electrical-power from Universiti Teknologi Malaysia (UTM), in 2009 and PhD degree from UniMAP, in 2022. He is currently a Lecturer with the Faculty of Electrical Engineering Technology, UniMAP. His research interests include artificial intelligence and optimization, power systems, power electronics, high voltage, and renewable energy.

Hedzlin Zainuddin received her B. Sc in Physics from Universiti Kebangsaan Malaysia in the year 2000. She obtained her M. Sc in Photovoltaics Energy System from the same university in the year 2003. In 2014, she completed her PhD in photovoltaics from Universiti Teknologi MARA, Shah Alam, Malaysia. Her specialization areas are physics, solar photovoltaic (PV) field testing, design of grid-connected PV (GCPV) system, design of off-grid PV (OGPV) system, mathematical and computational modeling (linear, multiple linear and artificial intelligent) and PV system fault detection. She presently holds four certificates of competency in GCPV and OGPV. She has been working with Industries and Government Agencies for 13 years since 2007 through consultation projects.

Ismail Bin Musirin obtained Bachelor of Electrical Engineering (Hons) in 1990 from Universiti Teknologi Malaysia, MSc Pulsed Power Technology in 1992 from University of Strathclyde, United Kingdom and PhD in Electrical Engineering from Universiti Teknologi MARA (UiTM), Malaysia in 2005. He is currently a Professor of Power System at the Faculty of Electrical Engineering, UiTM and headed the Power System Operation (POSC) Computational Intelligence Research Group. He has authored 2 books published, over 350 papers in international indexed journals and conferences. He is also an international journal reviewer for IEEE Transactions, Elsevier Science, WSEAS, John Wiley, IET and some other publishers. He has chaired more than 20 international conferences since 2007. To date, he has delivered keynote speeches at Cambridge University, United Kingdom, Dubai, Korea and Malaysia. He has also been given opportunity to evaluate research grants at the national and international levels. His research interest includes Artificial Intelligence, Optimization Techniques, Power System Analysis, Renewable Energy, Distributed Generation and Power System Stability. He is a professional engineer and a senior member of International Association of Computer Science and Information Technology (IACSIT), member of Artificial Immune System Society (ARTIST) and member of International Association of Engineers (IAENG), Hong Kong.